

Automated Reservoir Extraction from Remotely Sensed Satellite Images

1. Introduction

The delineation and extraction of inland water bodies is an important task in many disciplines, including lake coastal zone management, coastline change and erosion monitoring, flood prediction, and water resource evaluation (Ouma & Tateishi, 2006; Sarp & Ozcelik, 2017). When using traditional ground surveying techniques and manual digitisation this task can be difficult, time-consuming and monotonous (Paul et al., 2013), especially if a region as large as a country or continent is considered. This is because water bodies can have complex shorelines, be very large, and may be inaccessible. Additionally, for applications within coastline change and erosion mapping, the extent of the water body must be regularly updated, emphasising the importance of an easily replicable technique.

Consequently, the extraction of water bodies from satellite images using an automated process has been increasingly used in recent years to overcome the issues associated with traditional methods (e.g. Shah, 2011; Verpoorter et al., 2012; Li et al., 2014; Sarp & Ozcelik, 2017).

The objective of this research is to use satellite imagery and a number of image processing techniques to extract reservoirs. The results from 10 images will be presented along with a critical discussion of the method, underpinned by an accuracy assessment. Finally, a case study of 3 satellite images of Lake Mead in 1984, 2002 and 2016 will be used to show the potential of this method to demonstrate reservoir change over time. This specific example is chosen as the effects of climate change upon Lake Mead's extent is often discussed (e.g. Barnett & Pierce, 2008; Forsythe et al., 2012).

2. Methodology

2.1 Satellite Images

The images used were taken from Google Earth and were each deliberately chosen to represent a range of conditions in order to test the limits of this method. This includes a variation in site location, leading to varying external environments, most

notably green fields vs. arid deserts, image resolutions and scale, and reservoir characteristics.

2.2 Extraction Technique

The method used to extract each reservoir consists of three main groups of image processing algorithms: image preparation, threshold-based segmentation, and edge-based segmentation. The image preparation algorithms aim to suppress noise found in the image. The threshold-based segmentation algorithms divide the image into regions based on colour and then through applying a threshold. Finally, the edge-based segmentation algorithms find the reservoir's shoreline and trace this edge into contour lines removing any small areas that were incorrectly found.

2.2.1 *Image Preparation*

The main purpose of this stage is to filter the noise and speckle in the hope of reducing noisy edges in for subsequent edge detection. In order to preserve the precise position of the reservoir edge, an edge-preserving operator is required to remove noise (Liu & Jezek, 2004). In this case a bilateral filter was chosen as it provides edge-preserving smoothing by means of a nonlinear combination of nearby image values (Tomasi & Manduchi, 1998). Before deciding upon this filter, various others were trialled (Figure 1).

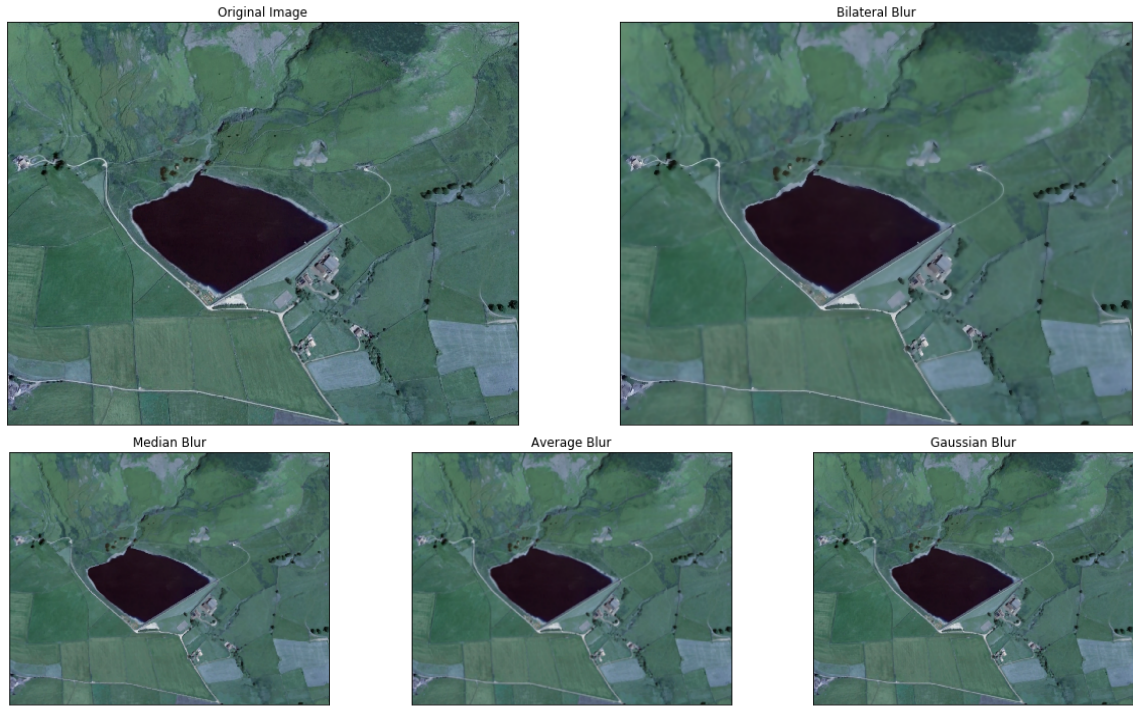


Figure 1: A trial using ‘res1.jpg’ to determine the smoothing filter. This trial was done using a number of images and the bilateral filter was deemed most effective. No salt and pepper noise was observed in any image used, so a median filter was not deemed necessary.

2.2.2 Threshold-based Segmentation

These algorithms aim to simplify the image into regions to provide meaningful information and highlight the reservoir. Gupta and Bora (2016) argue this is the most important and critical part of image analysis processes.

Firstly, a clustering technique, the K-Means algorithm, was used to divide the image into a given number (K-value) of colour regions. This algorithm is often observed to suffer from over segmentation due to an unsuitable K-value (Tariq & Burney, 2014; Gupta & Bora, 2016). Consequently, the K-value of 9 was chosen after extensive trial and error.

Next, the segmented image was converted to greyscale to use thresholding to create a mask. In this case two thresholding algorithms were applied: the ‘in range’ function and the Otsu method. The ‘in range’ function specifies the colour range to be masked. As the image was converted to greyscale, the deep-water reservoirs generally showed up as the darkest values, which in most cases was black (Figure 2). Therefore, after trial and error the optimum threshold range was found to be 0-30

(Figure 2). The Otsu algorithm then further refined this mask by iterating through all possible threshold values and calculating the optimum value.

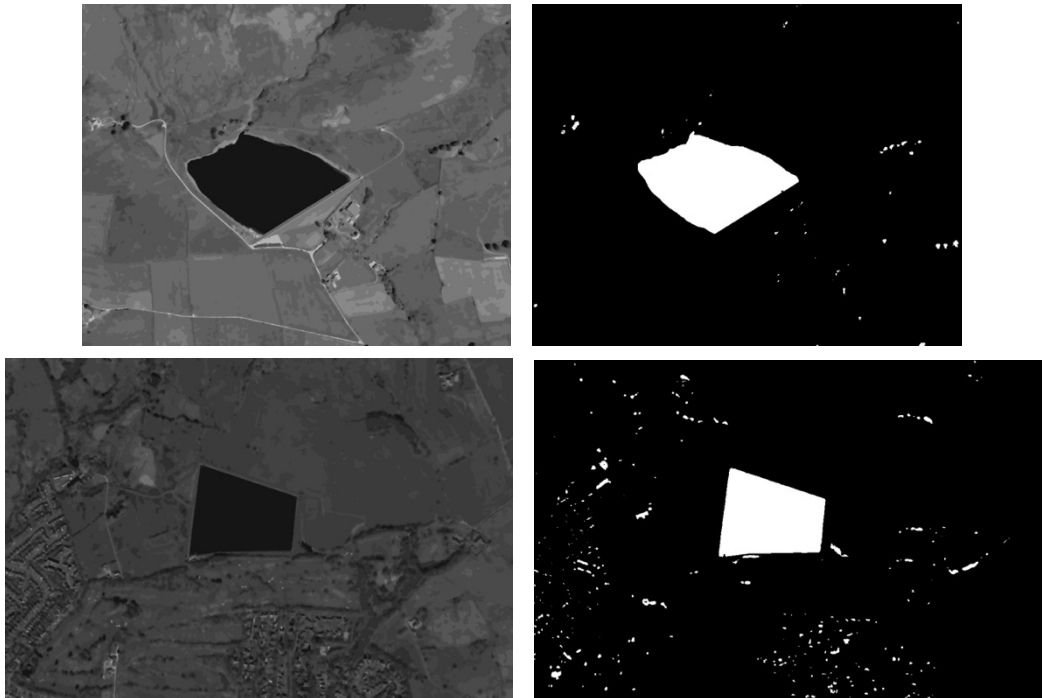


Figure 2: The grayscale K-means images of 'res1.jpg' and 'res4.jpg' showing the reservoirs to be the darkest shades of the image (left) and the masked images after carrying out thresholding (right).

2.2.3 Edge-based Segmentation

In order to identify the feature from the image, the algorithms in this section aim to find the reservoir's edge and convert these edges into contour lines.

To find the edges the Canny edge detector was applied. It was chosen as it was the most effective edge detector compared to Sobel and Laplacian. Additionally, it was used to effectively detect coastlines automatically in other research (Liu & Jezek, 2004; Xu-kai et al., 2012), a process drawing similarities with detecting reservoirs. The success of the Canny method may be due to its five-stage approach. A morphological transformation, dilation, was then applied to improve edge quality (Figure 3).

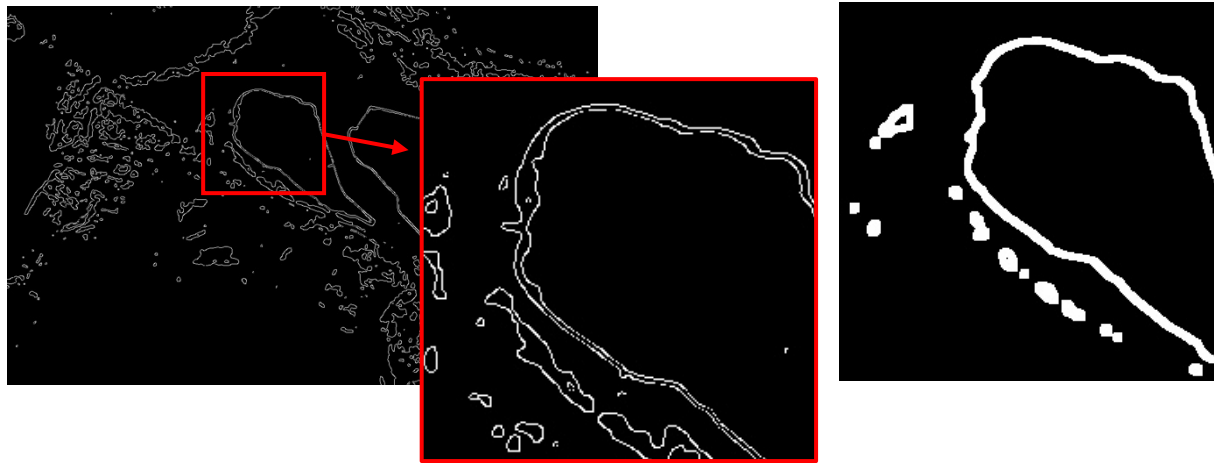


Figure 3: The results of using the Canny edge detector on image ‘res3.jpg’ before (left) and after (far right) applying a dilation transformation. This helped to enlarge edges and repair breaks. These images show a vast improvement to the quality of the lines detected after dilation.

Contours were then found using the ‘find contours’ tool. Contours are a curve joining every continuous point along any given boundary, which have the same colour or intensity. In this case, contours are useful for quality assessment as their area can be calculated and the smallest contours, which are assumed to be noise, can be removed.

2.3 Accuracy

To assess if the reservoir(s) in the image have been accurately extracted, the Intersection over Union (IoU) evaluation method was implemented. This works by comparing two bounding boxes: the ground-truth bounding box representing the actual reservoir area; and predicted bounding box, which is the largest bounding box from those drawn around the contours. The largest bounding box was used as it is assumed to contain the reservoir. The ground-truth boxes were generated using the program ‘labelImg’.

The IoU metric is then calculated by computing the area of overlap between the two bounding boxes, the area of union, and then dividing the former by the latter. Generally, any score higher than 0.5 is considered a good prediction.

3. Results

The accuracy assessment results and final output images are seen in Table 1. Additionally, output images for each stage can be seen for one image in Figure 4.

Despite two failed cases (*res5.jpg* and *res9.jpg*), the accuracy results are almost all good predictions. It is important to note, however, that despite a good accuracy assessment, many outputs contain noise. For example, '*res2.jpg*' has a good accuracy, with the reservoir correctly identified, but the image contains many incorrectly extracted contours. This is likely due to the image containing shadows (Figure 5). Therefore, extensive manual clean-up would be needed.



Figure 5: The original '*res2.jpg*' image (left) and a zoomed in portion to show shadows caused by trees (right). These shadows are a main cause of incorrectly extracted contours as their colour reflectance matches that of the reservoir after carrying out thresholding.

On the other hand, '*res7.jpg*' not only had a high accuracy, but generated no incorrect extractions with only 2 contours found, representing the reservoir. The results for this image contained more noise, with 13 contours being identified, when the smallest contours were not removed. Therefore, this step is vital for improving accuracy.

The results generated from '*manyres.jpg*' are somewhat misleading. The accuracy assessment, 0.0387, gives the impression that the reservoirs are not correctly extracted. However, when looking at the image, despite some incorrect contours, each reservoir appears to be successfully identified. This is an issue with the accuracy assessment only considering the biggest bounding box, as the method was not optimised for images containing more than one reservoir. This can also be seen in '*res3.jpg*'.

For further testing, the method was adjusted for the images with no output by altering the threshold range to 0-40 (Figure 6). For ‘res5.jpg’ the results were somewhat good, however for ‘res9.jpg’ poor results were still generated.

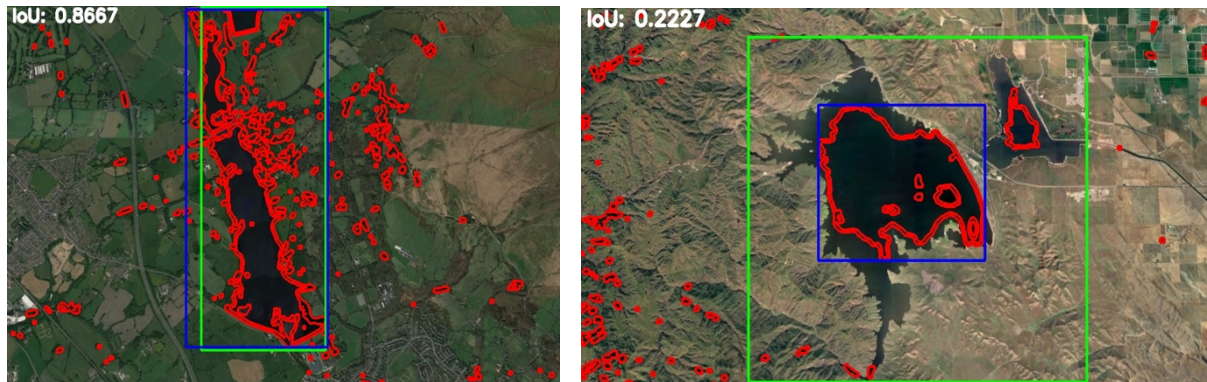


Figure 6: The images where there was no initial output generated after changing the threshold range to 0-40: ‘res5.jpg’ (left) and ‘res9.jpg’ (right).

The case study using satellite images of Lake Mead in 1984, 2002 and 2016 shows the potential for demonstrating reservoir extent over time (Figure 7). The image does contain noise, incorrect extractions and the reservoir outline may not be completely accurate, meaning they could not be used for quantitative assessment, however the image provides a compelling visual.

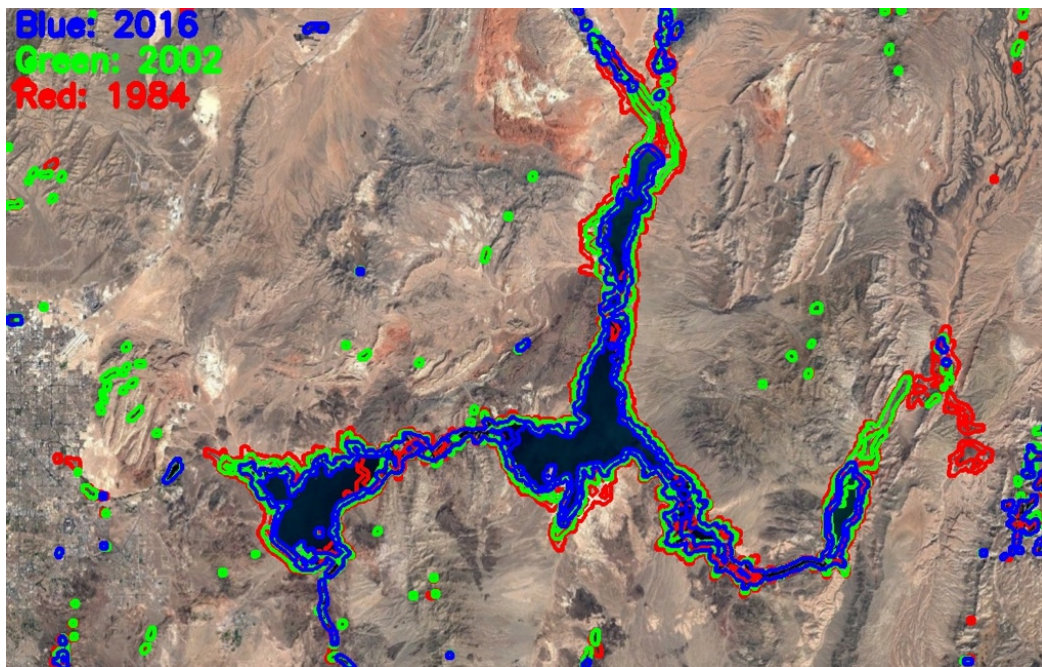
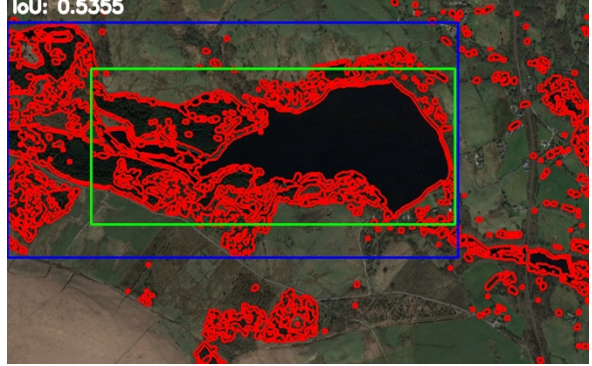
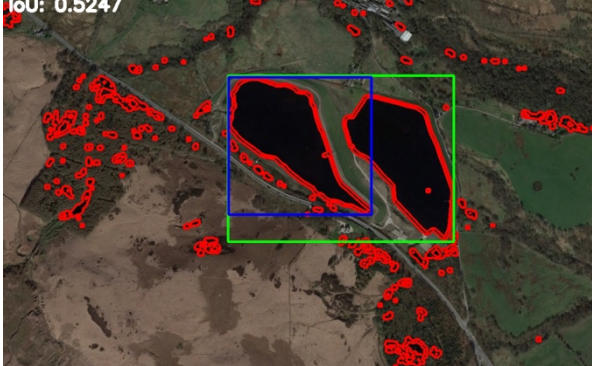
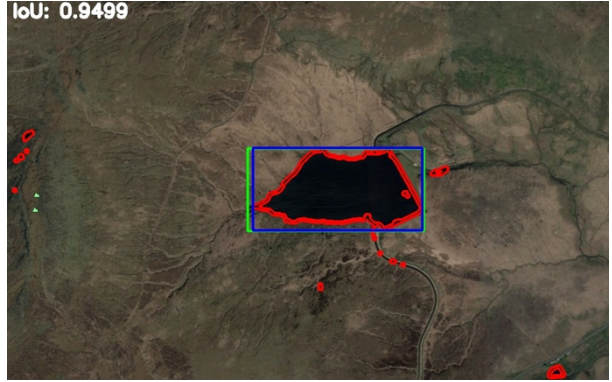
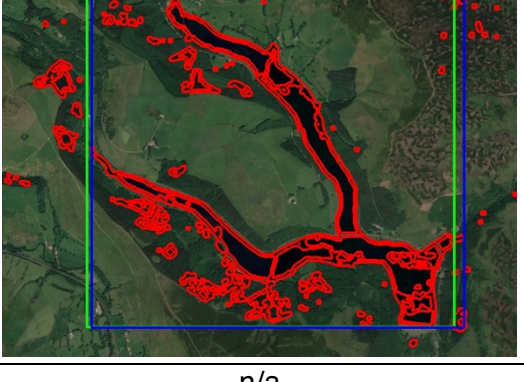


Figure 7: The extent of Lake Mead extracted automatically using this method from satellite images taken in 2016 (blue), 2002 (green) and 1984 (red) layered over the image of Lake Mead from 2016.

Table 1: A table displaying image name, the calculated IoU value to show accuracy, and the final image. The final image shows the generated contours in red, predicted bounding box in blue, and the ground-truth bounding box in green.

Image Name	Calculated IoU value	Final Image
Res1.jpg	0.9627	
Res2.jpg	0.5355	
Res3.jpg	0.5247	
Res4.jpg	0.9280	

SLLM7

Res5.jpg	0	n/a
Res6.jpg	0.9499	 IoU: 0.9499
Res7.jpg	0.9610	 IoU: 0.9610
Res8.jpg	0.9328	 IoU: 0.9328
Res9.jpg	0	n/a
Manyres.jpg	0.0387	 IoU: 0.0387

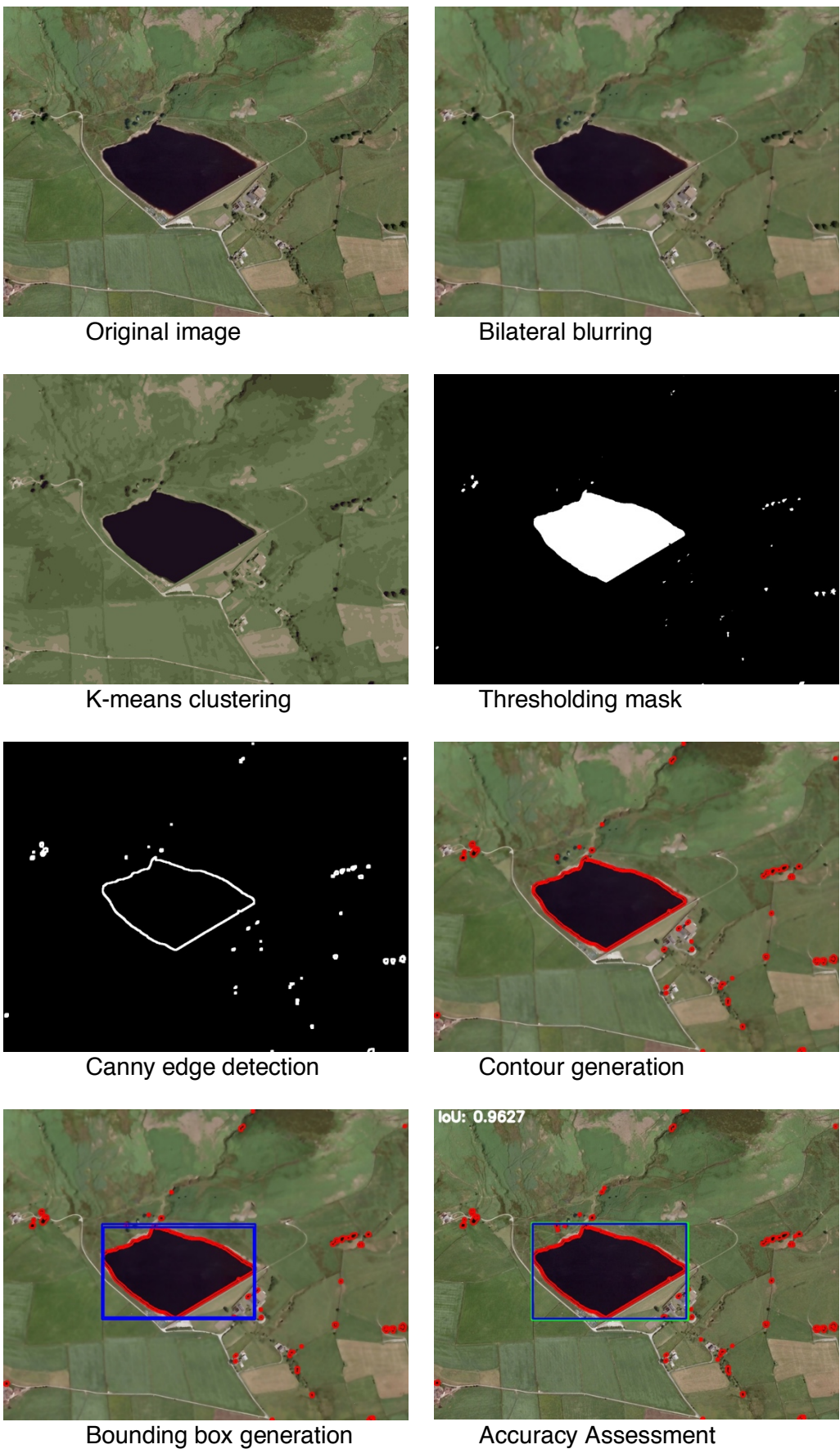


Figure 4: The output images for ‘res1.jpg’ after each stage of the method.

4. Discussion

In terms of extracting the reservoir(s) in each image, despite two failures, the proposed solution worked well. This is largely due to the threshold-based segmentation stage, where the image was divided into colour regions and masked. Due to extensive trial and error, the K-value for the K-means clustering and the value for thresholding was generally optimal, making the results as successful as possible.

Additionally, the use of dilation in conjunction with the Canny edge detector drastically improved results. In preliminary findings, the edges detected were thin and disconnected, therefore very few contours were identified. After incorporating dilation, the contours were more easily found, leading to higher success.

However, despite the reservoirs being successfully extracted, with exception of ‘res7.jpg’, there were many incorrect extractions in each image. This means that the contours generated would need be cleaned up manually or the method further refined. In their research on automated mapping of glacial outlines, Paul et al. (2013) found automated mapping was preferable to manual digitisation, however manual was recommended for correcting inaccuracies, similar to what could occur with this method.

In many cases incorrect extractions came from dark areas in the images, such as small areas of water, woodland, and shadows. Li et al. (2014) commented on how shadows in images are typical noise for water extraction, as it becomes difficult to distinguish between the two. McFeeters (1996) found water information mixing with shadows in images often led to an overestimation or underestimated of extracted open water.

For the two cases with no output, it can be seen that in original images the reservoirs both had overhead noise, thus influencing the segmentation due to changing the reflectance of the reservoir’s surface (Figure 8). Brown and Young (2006) note that the incident angle of the sun may cause specular reflection of sunlight on the water’s surface making it difficult to differentiate water from other areas when using the visible spectrum. Vegetation cover on the water surface, water turbidity, and cloud cover have also been identified as problems for thresholding (Yoshikawa & Hinzman, 2003; Brown & Young, 2006; Hui et al., 2008). Each of these issues may explain why the two images within this research led to no successful extraction until threshold values were altered.



Figure 8: The images where there was no initial output generated: ‘res5.jpg’ (top) and ‘res9.jpg’ (bottom). It can be seen in the zoomed inset images (right) that each reservoir surface was subject to noise. This was likely why the thresholding section of the method did not detect the reservoir as the colour would have been affected.

Consequently, to improve the method, different parts of the electromagnetic spectrum may be considered. Baban (1999) notes that within the near infrared band there is high contrast between reflectance characteristics of land and water. Furthermore, many papers involving extraction of water bodies and floods have been successful when thresholding in infrared bands (Jupp et al., 1985; McFeeters, 1996; Wang et al., 2002; Hui et al., 2008). Therefore, incorporating infrared may be a future improvement.

In addition to spectral information, geometric features, such as shape (e.g. Li, 1995), water surface texture (e.g. Sivanpillai & Miller, 2010) and topographic information, such as DEM data (e.g. Wang et al., 2002) can also be used to enhance water extraction (Sun et al., 2012). To improve this method, therefore, any one of these could be integrated.

Finally, although in many cases the reservoir edge was extracted, the accuracy of the shoreline shape is likely not a realistic representation. In order to improve accuracy, images of a higher spatial resolution would need to be used, following Shah (2011). Furthermore, with an improvement to shoreline accuracy, a quantitative figure may be able to be generated showing reduction in reservoir extent over time, such as that of Lake Mead.

5. Conclusion

To conclude, the method outlined provides a somewhat successful process to extract reservoirs from satellite images. The method uses a combination of image processing techniques, including threshold-based and edge-based segmentation. Despite issues with the accuracy assessment, accuracy results are pleasing for the images where extraction did not fail. However, incorrect extraction caused by noise in the images, such as shadows, small areas of water, or thick vegetation, leads to problems. Consequently, to be used on additional images and other scenarios, the method would need refinement, as outlined in the discussion. Finally, the method proved beneficial in providing a visual demonstration of the reduction in Lake Mead's extent over time, which has potential to be applied in other case studies, however, the accuracy would need to be improved in order to provide quantitative data.

References

- Baban, S. (1999) 'Use of remote sensing and geographical information systems in developing lake management strategies', In *The Ecological Bases for Lake and Reservoir Management*, Developments in Hydrobiology, Springer, Dordrecht, pp. 211–226
- Barnett, T. and Pierce, D. (2008) 'When will Lake Mead go dry?', *Water Resources Research*, 44(3)
- Brown, L. and Young, K. (2006) 'Assessment of Three Mapping Techniques to Delineate Lakes and Ponds in a Canadian High Arctic Wetland Complex', *Arctic*, 59(3), pp. 283–293.
- Forsythe, K., Schatz, B., Swales, S., Ferrato, L. and Atkinson, D. (2012) 'Visualization of Lake Mead Surface Area Changes from 1972 to 2009', *ISPRS International Journal of Geo-Information*, 1(2), pp. 108–119.
- Gupta, A. and Bora, D. (2016) 'A Novel Color Image Segmentation Approach Based On K-Means Clustering with Proper Determination of the Number of Clusters and Suitable Distance Metric', *International Journal of Computer Science & Engineering Technology*, 7, pp. 395–409.
- Hui, F., Xu, B., Huang, H., Yu, Q. and Gong, P. (2008) 'Modelling spatial-temporal change of Poyang Lake using multitemporal Landsat imagery', *International Journal of Remote Sensing*, 29(20), pp. 5767–5784.
- Jupp, D., Mayo, K., Kuchler, D., Heggen, S. and Kendall, S. (1985) *Landsat based interpretation of the cairns section of the great barrier reef marine park.*, The CSIRO Natural Resource Series.
- Li, B., Zhang, H. and Xu, F. (2014) 'Water Extraction in High Resolution Remote Sensing Image Based on Hierarchical Spectrum and Shape Features', *IOP Conference Series: Earth and Environmental Science*, 17(1), p. 012123.
- Li, X. (1995) 'A new method to improve classification accuracy with shape information.', *Journal of Remote Sensing*, 10, pp. 279–287.
- Liu, H. and Jezek, K. (2004) 'Automated extraction of coastline from satellite imagery by integrating Canny edge detection and locally adaptive thresholding methods', *International Journal of Remote Sensing*, 25(5), pp. 937–958.
- McFeeters, S. (1996) 'The use of the Normalized Difference Water Index (NDWI) in the delineation of open water features', *International Journal of Remote Sensing*, 17(7), pp. 1425–1432.
- Ouma, Y. O. and Tateishi, R. (2006) 'A water index for rapid mapping of shoreline changes of five East African Rift Valley lakes: an empirical analysis using Landsat TM and ETM+ data', *International Journal of Remote Sensing*, 27(15), pp. 3153–3181.

- Paul, F., Barrand, N., Baumann, S., Berthier, E., Bolch, T., Casey, K., Frey, H., Joshi, S., Konovalov, V., Bris, R., Mölg, N., Nosenko, G., Nuth, C., Pope, A., Racoviteanu, A., Rastner, P., Raup, B., Scharrer, K., Steffen, S. and Winsvold, S. (2013) 'On the accuracy of glacier outlines derived from remote-sensing data', *Annals of Glaciology*, 54(63), pp. 171–182.
- Sarp, G. and Ozcelik, M. (2017) 'Water body extraction and change detection using time series: A case study of Lake Burdur, Turkey', *Journal of Taibah University for Science*, 11(3), pp. 381–391.
- Shah, C. (2011) 'Automated Lake Shoreline Mapping at Subpixel Accuracy', *IEEE Geoscience and Remote Sensing Letters*, 8(6), pp. 1125–1129.
- Sivanpillai, R. and Miller, S. (2010) 'Improvements in mapping water bodies using ASTER data', *Ecological Informatics*, 5(1), pp. 73–78.
- Sun, F., Sun, W., Chen, J. and Gong, P. (2012) 'Comparison and improvement of methods for identifying waterbodies in remotely sensed imagery', *International Journal of Remote Sensing*, 33(21), pp. 6854–6875.
- Tariq, H. and Burney, S. (2014) 'K-Means Cluster Analysis for Image Segmentation', *International Journal of Computer Applications*, 96.
- Tomasi, C. and Manduchi, R. (1998) 'Bilateral filtering for gray and color images', In *Sixth International Conference on Computer Vision (IEEE Cat. No.98CH36271)*, pp. 839–846.
- Verpoorter, C., Kutser, T. and Tranvik, L. (2012) 'Automated mapping of water bodies using Landsat multispectral data', *Limnology and Oceanography: Methods*, 10(12), pp. 1037–1050.
- Wang, Y., Colby, J. and Mulcahy, K. (2002) 'An efficient method for mapping flood extent in a coastal floodplain using Landsat TM and DEM data', *International Journal of Remote Sensing*, 23(18), pp. 3681–3696.
- Xu-kai, Z., xia, Z., Qiong-qiong, L. and Baig, M. (2012) 'Automated detection of coastline using Landsat TM based on water index and edge detection methods', In *2012 Second International Workshop on Earth Observation and Remote Sensing Applications*, pp. 153–156.
- Yoshikawa, K. and Hinzman, L. (2003) 'Shrinking thermokarst ponds and groundwater dynamics in discontinuous permafrost near council, Alaska', *Interations of Permafrost with Climatic, Hydrologic and Ecosystem Processes*, 14(2), pp. 151–160.